Research on Output Feedback Guaranteed Performance Control for Dual-pickup ICPT System Based on D-LCL Compensation

Xin Li, Wen-li Gao, and Hao Wang

***Abstract*—The high-power high-frequency dual-pickup inductively coupled power transfer (ICPT) system has high-order resonant characteristics and is highly sensitive to changes in system parameters. It is necessary to overcome the influence of parameter uncertainty on the system. In this paper, the dual-pickup ICPT system based on the D-LCL compensation circuit adopts the output feedback guaranteed performance control, which ensures the robustness of the parameter uncertainty system while ensuring the boundedness of its performance index. Firstly, establishing the dynamic model of the system, on this basis, the parameter uncertainties are introduced to form the uncertainty system model. Then, using the linear matrix inequality (LMI) method, the guaranteed performance controller of the uncertain parameter system is designed, this paper givens the necessary and sufficient conditions for the existence of the output feedback guaranteed performance controller. Finally, the LMI Control Toolbox in MATLAB is used to verify that the control method can ensure the system has excellent robust stability and performance robustness, and the system has excellent tracking performance when the parameters change.**

***Index Terms*—D-LCL compensation, dual-pickup ICPT system, parameter uncertainty, guaranteed performance control, linear matrix inequality (LMI).**

I. Introduction

THE dual-pickup inductively coupled power transfer (ICPT) system realizes power transfer from the stationary grid side to multiple mobile devices contactless based on the principle of electromagnetic induction, high-power high-frequency inverter technology and resonance compensation technology [1]. The dual-pickup ICPT technology can increase the reliability and safety of power supply, improve the power capacity of the system, and meet the occasions with high power requirements [2]-[4]. The fields of power supply, including high-power electric vehicles, trams and high-speed railway trains [5]-[9], has used the ICPT technology. This paper gives a particular focus to the study of the dual-pickup ICPT system with rail transport as the application background.

In the dual-pickup ICPT system, the loosely coupled transformer has a low coupling coefficient and the large leakage inductance, resulting in higher reactive power and lower transmission efficiency during transmission. To reduce reactive power, unnecessary loss and improve the power supply capacity, some scholars have done much research. Bertoluzzo et al. [10]-[13] proposed to optimize the design of the magnetic coupling mechanism or to increase the compensation circuit of the primary and secondary sides, and the method of adding the compensation circuit is more natural to implement. However, the traditional four compensation structures are challenging to achieve the goal of improving transmission efficiency, so many scholars have focused on hybrid compensation topologies like TS-S, LCC-S, LCC-P, D-LCC, and D-LCL. The TS-S circuit topology has good robustness, which can achieve constant output voltage and current without any control, increasing the adaptation range of the primary side equivalent load [12]. In addition to the characteristics of the constant voltage output, the LCC-S typed compensation structure is less sensitive to system frequency offset when the output resistance is massive [13]. But, the output power and transmission efficiency of the two compensation structures are low. D-LCC and LCC-P circuits are more suitable for low power applications with constant current output requirements [14]. Because the D-LCL compensation topology can achieve constant output current and voltage, with higher output power and transmission efficiency, it is more suitable for dual pick-up ICPT system with rail transit as the application background.

Because of the inaccuracy of the measurement devices and manufacturing processes, there are some errors between the actual and theoretical electrical parameters of the resonant circuit components, which is known as the uncertainties of the dual-pickup ICPT system. The dual-pickup ICPT system has high-order resonance characteristics and is therefore very sensitive to uncertainty. Although the D-LCL compensation topology has excellent characteristics, it cannot solve the problem of system uncertainty. For this reason, based on the system parameter perturbation model using the generalized state-space averaging method, some scholars have proposed an H∞ robust controller that can suppress the mutual inductance perturbation by changing the gain of the output weighting function [15], [16]. Its control requirements for

Manuscript received June 18, 2019; revised August 29, 2019. This work was supported in part by the National Natural Science Foundation of China (project no.: 51767015), the Gansu Provincial Natural Science Foundation of China (Gansu Provincial Science and Technology Plan; project no.: 18JR3RA117) and Lanzhou Jiaotong University-Tianjin University Joint Innovation Fund Project (project no.: 2019051).

Xin Li is with the College of New Energy and Power Engineering Lanzhou Jiaotong University, Lanzhou, China (corresponding author; e-mail: lxfp167@163.com).

Wen-li Gao is with Key Laboratory of Opto-Electronic Technology and Intelligent Control Ministry of Education of Lanzhou Jiaotong University, Lanzhou, China (e-mail: 1715724401@qq.com).

Hao Wang is with Key Laboratory of Opto-Electronic Technology and Intelligent Control Ministry of Education of Lanzhou Jiaotong University, Lanzhou, China (e-mail: 943908531@qq.com).

uncertainties are limited to robust stability, ignoring the requirements of the system for related robust performance. The guaranteed performance control can achieve the robust stability of the system while ensuring its performance index does not exceed an absolute upper bound [17]-[19]. Therefore, the output feedback guaranteed performance control is adopted through this paper to the parameter uncertainty problem of D-LCL compensated dual-pickup ICPT system, which ensures the robust stability of the uncertain system while getting its performance robustness. Output feedback control can solve the problem that the system state variable is unknown, and it is difficult to obtain state estimation [20]. By using the LMI method to solve the output feedback guaranteed performance controller, the design problem of the controller can be easily transformed into the problem of solving the feasible solution of LMI [21], [22], thus ensuring the robust stability and performance robustness of the system.

This paper is organized as follows. In Section II, the transmission characteristics of D-LCL compensated ICPT system are briefly analyzed, and describes the dual pick-up ICPT system based on D-LCL compensation. The dynamic model of the system is established by the state-space method, and the parameter uncertainty is introduced to establish the system uncertainty model. In Section III, design the output feedback guaranteed performance controller by using Schur complement lemma, variable substitution method and LMI. And give the necessary and sufficient conditions for the existence of quadratic cost matrix P and output feedback guaranteed performance controller. Section IV uses the LMI Control Toolbox in MATLAB to find the output feedback guaranteed performance controller and the upper bound of the quadratic performance index and makes the impulse response curves of the closed-loop systems with the nominal model and the uncertainty model respectively. The simulation shows that the system has excellent robust stability and performance robustness.

II. Dual-pickup ICPT System based on D-LCL Compensation

A. Analysis of Transmission Characteristics of ICPT System Based on D-LCL Compensation

In the ICPT system, to improve the frequency robustness, filter the harmonics generated by the inverter during the working process, and adjust the transmission power and efficiency of the system when the load is stationary, the compensation of the primary and secondary sides usually adopts a hybrid compensation topology. Common hybrid compensation topologies include D-LCC, LCC-S, LCC-P, TS-S, and D-LCL. The schematic diagrams of the above five hybrid compensation topologies are shown in Figs.1 to 5. U and I_1 are the input voltage and current of the compensation circuits. L_{f1}, L_P, C_{f1} and C_1 are the filter inductances and capacitors on the primary side, respectively, and L_{f2}, C_{f2} and C_2 differ from them in that they are on the secondary. The transmitting coil L_1 and the receiving coil L_2 form a transformer. I_2, I_3 and I_4 are the current values flowing through the coils L_1, L_2 and the load R_L, respectively. M represents the mutual inductance between L_1 and L_2.

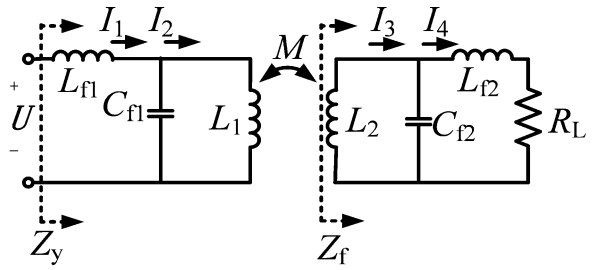

Fig. 1. D-LCL typed compensation topology

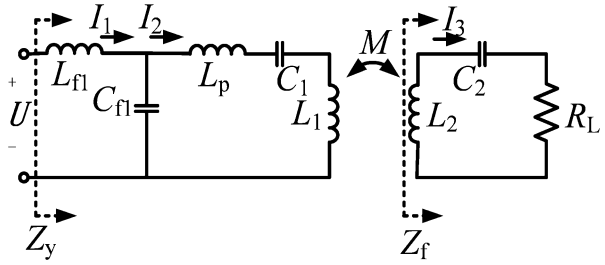

Fig. 2. TS-S typed compensation topology

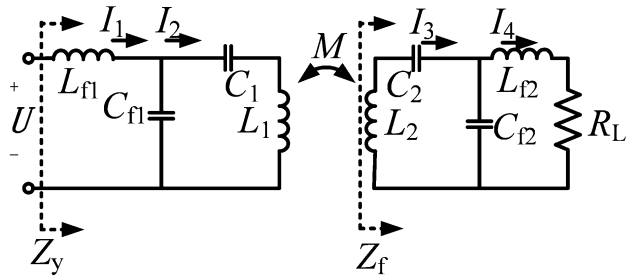

Fig. 3. D-LCC typed compensation topology

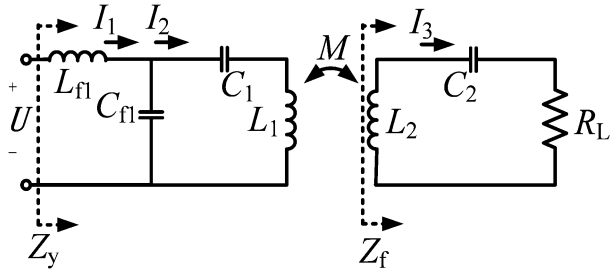

Fig. 4. LCC-S typed compensation topology

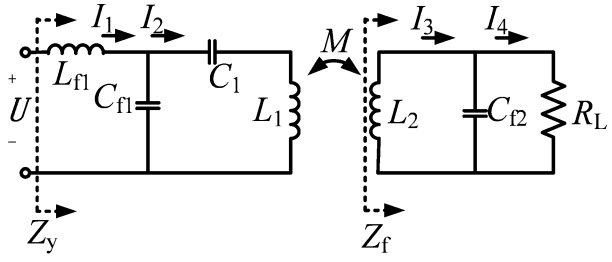

Fig. 5. LCC-P typed compensation topology

In Fig. 1, the voltage across the load is

$$U_{\text{out}} = \frac{MU}{L_{f1}\lambda}$$

According to G. M. Xu et al. [20], the output power of the system can be calculated by:

$$P_{\text{out}} = \frac{M^2 U^2}{L_{\text{f}1}^2 \lambda^2 R_{\text{L}}}$$

The transmission efficiency of the system is given by:

$$\eta = \frac{M^2 \operatorname{Re}\left(Z_{\text{y}}\right)}{L_{\text{f}1}^2 \lambda^2 R_{\text{L}}}.$$

In Figs. 2 to 5, Z_{f} is the pick-up impedance. Z_{y} is the total input impedance. Obtaining from the impedance relationship of the circuit, the total impedance Z_{f} on the secondary side is

$$Z_{\text{f}} = \text{j}wL_2 + \frac{1}{\text{j}wC_2} + \frac{\frac{1}{\text{j}wC_{\text{f}2}}(\text{j}wL_{\text{f}2} + R_{\text{L}})}{\frac{1}{\text{j}wC_{\text{f}2}} + \text{j}wL_{\text{f}2} + R_{\text{L}}} \tag{2.1}$$

The impedance Z_{r} reflected from the pickup side to the primary side is

$$Z_{\text{r}} = \frac{w^2 M^2}{Z_{\text{f}}} \tag{2.2}$$

The total impedance Z_{y} on the primary side is

$$Z_{\text{y}} = \text{j}wL_{\text{f}1} + \frac{\frac{1}{\text{j}wC_{\text{f}1}}\left(\text{j}wL_{\text{p}} + \frac{1}{\text{j}wC_1} + \text{j}wL_1 + Z_{\text{r}}\right)}{\text{j}wC_{\text{f}1} + \text{j}wL_{\text{p}} + \frac{1}{\text{j}wC_1} + \text{j}wL_1 + Z_{\text{r}}} \tag{2.3}$$

Following Kirchhoff's law, we can get

$$\begin{aligned}
&U = \text{j}wL_{\text{f}1}I_1 + \frac{1}{\text{j}wC_{\text{f}1}}(I_1 - I_2)\\
&0 = \frac{1}{\text{j}wC_{\text{f}1}}I_1 - \left(\frac{1}{\text{j}wC_{\text{f}1}} + \frac{1}{\text{j}wC_1} + \text{j}wL_1 + \text{j}wL_{\text{p}}\right)I_2 + \text{j}wMI_3\\
&\begin{cases}
\begin{cases}
0 = \text{j}wMI_2 - (\text{j}wL_2 + \frac{1}{\text{j}wC_2} + \frac{1}{\text{j}wC_{\text{f}2}})I_3 + \frac{1}{\text{j}wC_{\text{f}2}}I_4\\
0 = \frac{1}{\text{j}wC_{\text{f}2}}I_3 - (\frac{1}{\text{j}wC_{\text{f}2}} + \text{j}wL_{\text{f}2} + R_{\text{L}})I_4
\end{cases}, I_4 \neq 0\\
0 = \text{j}wMI_2 - (\text{j}wL_2 + \frac{1}{\text{j}wC_2} + R_{\text{L}})I_3, I_4 = 0
\end{cases}
\end{aligned} \tag{2.4}$$

If there is no C_{i} or L_{j} in Fig. 1, the terms associated with C_{i} or L_{j} from the impedance expressions and the Kirchhoff voltage equations equal 0 (i=1, 2, f2, j=p, f2). The necessary and sufficient condition for the full resonance of the system can be obtained from (2.5).

$$\begin{cases}
L_{\text{f}1} = \frac{1}{C_{\text{f}1}w^2}\\
L_1 = \frac{1}{(C_{\text{f}1} + C_1)w^2}\\
L_2 = \frac{1}{C_2 w^2}
\end{cases}, \text{(LCC-S/ LCC-P)}, \begin{cases}
L_{\text{f}1} = \frac{1}{C_{\text{f}1}w^2}\\
L_1 = \frac{1}{(C_{\text{f}1} + C_1)w^2}\\
L_{\text{f}2} = \frac{1}{C_{\text{f}2}w^2}\\
L_2 = \frac{1}{(C_{\text{f}2} + C_2)w^2}
\end{cases}, \text{(D-LCC)},$$

$$\begin{cases}
L_{\text{f}1} = \frac{1}{C_{\text{f}1}w^2}\\
L_1 = \frac{1}{C_1 w^2}\\
L_{\text{p}} = \frac{1}{C_{\text{f}1}w^2}\\
L_2 = \frac{1}{C_2 w^2}
\end{cases}, \text{(TS-S)} \tag{2.5}$$

Substituting (2.5) into (2.1)-(2.4), the expressions of primary current, secondary output voltage, output power and efficiency under the condition of complete resonance are given by:

$$\begin{cases}
I_2 = \frac{U}{L_{\text{f}1}w}\\
U_{\text{out}} = \frac{MU}{L_{\text{f}1}}\\
P_{\text{out}} = \frac{M^2U^2}{L_{\text{f}1}^2 R_{\text{L}}}\\
\eta = \frac{M^2 \operatorname{Re}(Z_{\text{y}})}{L_{\text{f}1}^2 R_{\text{L}}}
\end{cases}, \text{(LCC-S)} \quad \begin{cases}
I_2 = \frac{U}{L_{\text{f}1}w}\\
U_{\text{out}} = \frac{MUR_{\text{L}}}{\text{j}L_{\text{f}1}L_2 w}\\
P_{\text{out}} = \frac{M^2U^2R_{\text{L}}}{L_{\text{f}1}^2 L_2^2 w^2}\\
\eta = \frac{M^2 \operatorname{Re}(Z_{\text{y}})}{L_{\text{f}1}^2 L_2^2 w^2}
\end{cases}, \text{(LCC-P)}$$

$$\begin{cases}
I_2 = \frac{U}{L_{\text{f}1}w}\\
U_{\text{out}} = \frac{MUR_{\text{L}}}{\text{j}L_{\text{f}1}L_{\text{f}2}w}\\
P_{\text{out}} = \frac{M^2U^2R_{\text{L}}}{L_{\text{f}1}^2 L_{\text{f}2}^2 w^2}\\
\eta = \frac{M^2 R_{\text{L}} \operatorname{Re}(Z_{\text{y}})}{L_{\text{f}1}^2 L_{\text{f}2}^2 w^2}
\end{cases}, \text{(D-LCC)} \quad \begin{cases}
I_2 = \frac{U}{L_{\text{f}1}w}\\
U_{\text{out}} = \frac{MU}{L_{\text{f}1}}\\
P_{\text{out}} = \frac{M^2U^2}{L_{\text{f}1}^2 R_{\text{L}}}\\
\eta = \frac{M^2 \operatorname{Re}(Z_{\text{y}})}{L_{\text{f}1}^2 R_{\text{L}}}
\end{cases}, \text{(TS-S)}$$

$$\begin{cases}
I_2 = \frac{U}{L_{\text{f}1}w}\\
U_{\text{out}} = \frac{MU}{L_{\text{f}1}\lambda}\\
P_{\text{out}} = \frac{M^2U^2}{L_{\text{f}1}^2 \lambda^2 R_{\text{L}}}\\
\eta = \frac{M^2 \operatorname{Re}\left(Z_{\text{y}}\right)}{L_{\text{f}1}^2 \lambda^2 R_{\text{L}}}
\end{cases}, \text{(D-LCL)} \tag{2.6}$$

It can be seen from (2.6) that the LCC-P and D-LCC typed hybrid compensation topologies realized the constant output current of the primary side. However, the output voltage of the secondary side varies as the load changes. LCC-S, TS-S and D-LCL typed compensation structures can realize the secondary side constant voltage while realizing the primary side constant current. The above analyses do not consider the influence of the parasitic resistances of the inductors. In practical applications, the parasitic resistances of the primary

and secondary resonant inductors are inevitable, the circuit parameters considering them are shown as follow:

TABLE I
THE CIRCUIT PARAMETERS

Parameter	LCC-S	LCC-P	D-LCC	TS-S	D-LCL
Voltage, U/V	400				
Resonant frequency, f/HZ	85300				
Coupling coefficient, k	0~0.5				
Primary coil, L_1/uH	120				
Secondary coil, L_2/uH	120				
Primary parasitic resistance, R_1/Ω	0.5				
Secondary parasitic resistance, R_2/Ω	0.5				
Primary capacitor, C_1/nF	29	29	44.15	29	-
Secondary capacitor, C_2/nF	44.15	44.15	44.15	29	-
Primary filter capacitor, C_{f1}/nF	84.6	84.6	84.6	29	29
Secondary filter capacitor, C_{f2}/nF	-	-	84.6	-	29
Primary filter inductor, L_{f1}/uH	41.15	41.15	41.15	120	120
Secondary filter inductor, L_{f2}/uH	-	-	41.15	120	120
Primary filter inductor, L_P/uH	-	-	-	120	-
Load resistance, R_L/Ω	10				

The five hybrid compensation topologies adopt the parameters shown in Table. I. As the coupling coefficient continues to increase, the output power and efficiency are shown in Figs. 6 to 7.

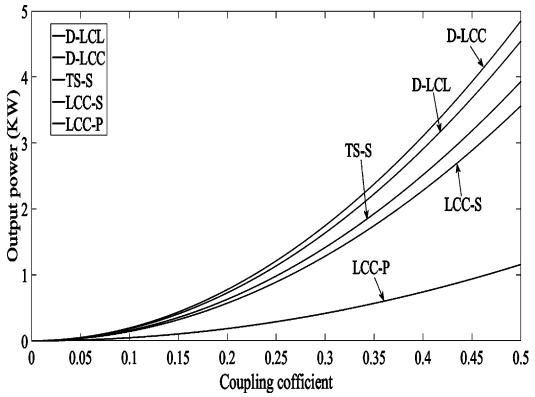

Fig. 6. Output power

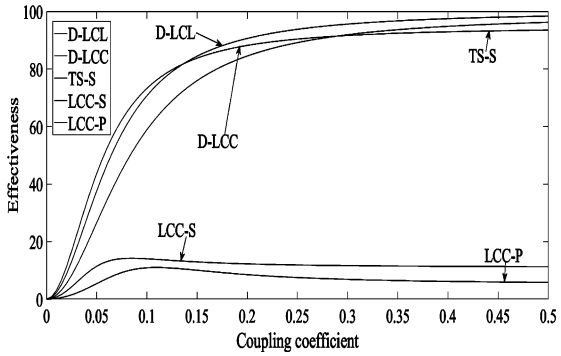

Fig. 7. Effectiveness

The simulation results show that the transmission efficiency of LCC-S and LCC-P typed compensation topologies is much lower than that of other compensation topologies. When the coupling coefficient exceeds 0.08 or 0.11, the efficiency even drops. When the coupling coefficient exceeds 0.17, the rising speed of the efficiency of the other three compensation topologies decreases, at this time, the efficiency has reached 80% or higher, and D-LCL typed compensation topology has the highest transmission efficiency. With the continuous increase of the coupling coefficient, the output power of the five compensation structures also rises. The output power of D-LCL and D-LCC is even more than 4KW, and they are relatively reliable compensation schemes. Considering that the stable output voltage is helpful for that dual pick-up ICPT system can be applied in the field of railway transportation, this paper uses D-LCL compensation structure.

B. Description for Dual-pickup ICPT System Based on D-LCL Compensation

The dual-pickup ICPT system based on D-LCL compensation is composed of two parts: the primary side and the secondary side, and the primary side includes high-frequency inverter and LCL resonance compensation network. Its basic structure is shown in Fig. 8. U and i_L are the high-frequency input voltage and current of the compensation circuit, respectively. L and C_P are the filter inductor and capacitor on the primary side, respectively. L_P、L_{S1} and L_{S2} are the transmitting coil and the two receiving coils, respectively. L_1、L_2、C_{S1} and C_{S2} are the filter inductors and capacitors on the secondary side, respectively. i_L、i_{LP}、i_{LS1}、i_{L1}、i_{LS2} and i_{L2} are current values flowing through L、L_P、L_{S1}、L_1、L_{S2} and L_2, respectively. R_L、R_P、R_{S1}、R_1、R_{S2} and R_2 are the equivalent internal resistances of L、L_P、L_{S1}、L_1、L_{S2} and L_2, respectively. M_1 and M_2 are the mutual inductance between the transmitting coil and the two pickup coils. C is the filter capacitor on the secondary side, R is the load on the secondary side.

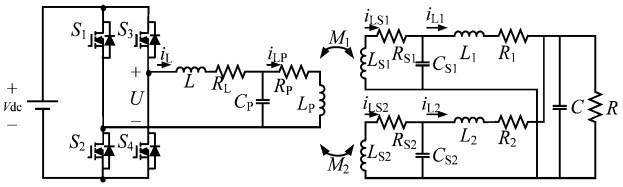

Fig. 8 Dual-pickup ICPT system based on D-LCL compensation

The induced voltage on the secondary side can be represented by the current on the primary side

$$v_{\mathrm{Lsi}}(t) = M_{\mathrm{i}} \frac{\mathrm{d}\, i_{\mathrm{Lp}}(t)}{\mathrm{d}\, t} \tag{2.7}$$

The voltage reflected from the secondary side to the primary side can be expressed as follow:

$$v_{\mathrm{ri}}(t) = -M_{\mathrm{i}} \frac{\mathrm{d}\, i_{\mathrm{Lsi}}(t)}{\mathrm{d}\, t} \tag{2.8}$$

Where M_{i} represents the mutual inductance between the transmitting coil L_{p} and the pick-up coils L_{si} (i=1, 2). The mutual inductance between the two pick-up coils is not considered.

C. The Establishment of The System Dynamic Model

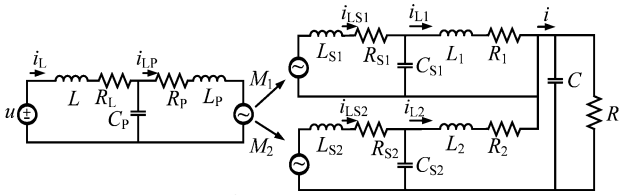

Fig. 9. Equivalent circuit of the ICPT system with D-LCL compensation and double pick-ups

The schematic diagram of the ICPT system with D-LCL compensation and double pick-ups is shown in Fig. 9, the specific steps to establish its dynamic model are as follows: (1) the selection of state variables: select the current/voltage on the inductors/capacitors as the state variables. (2) The equations based on Kirchhoff's law are further written in the form of a matrix. (3) Select the high-frequency input voltage U of the compensation circuit and the voltage u_c across the load R as the system input and output, respectively. The state-space description of the system can be obtained.

$$x = \begin{bmatrix} x_1 & x_2 & x_3 & x_4 & x_5 & x_6 & x_7 & x_8 & x_9 & x_{10} \end{bmatrix}^{\mathrm{T}}$$
$$= \begin{bmatrix} i_{\mathrm{L}} & u_{\mathrm{CP}} & i_{\mathrm{LP}} & i_{\mathrm{LS1}} & u_{\mathrm{CS1}} & i_{\mathrm{L1}} & i_{\mathrm{LS2}} & u_{\mathrm{CS2}} & i_{\mathrm{L2}} & u_{\mathrm{C}} \end{bmatrix}^{\mathrm{T}}$$

Where:

u_{cp}-voltage across the primary side filter capacitor C_P

u_{cs1}- voltage across the secondary side filter capacitor C_{S1}

u_{cs2} - voltage across the secondary side filter capacitor C_{S2}

u_c - voltage across the load R

Define the input vector of the system as follow:

$$U = [u]^{\mathrm{T}}$$

Following Kirchhoff's law, and we can get 10 differential equations as follows:

$$\dot{x}_1 = -\frac{R_{\mathrm{L}}}{L} x_1 - \frac{1}{L} x_2 + \frac{1}{L} u$$

$$\dot{x}_2 = \frac{1}{C_{\mathrm{P}}} x_1 - \frac{1}{C_{\mathrm{P}}} x_3$$

$$\dot{x}_3 = \frac{\gamma}{L_{\mathrm{P}}} x_2 - \frac{\gamma R_{\mathrm{P}}}{L_{\mathrm{P}}} x_3 - \gamma\beta_1 R_{\mathrm{s}1} x_4 - \gamma\beta_1 x_5 - \gamma\beta_2 R_{\mathrm{s}2} x_7 - \gamma\beta_2 x_8$$

$$\dot{x}_4 = \gamma\beta_1 x_2 - \gamma\beta_1 R_{\mathrm{P}} x_3 - \alpha_1 x_4 - \eta_1 x_5 - \sigma_1\beta_2 R_{\mathrm{s}2} x_7 - \sigma_1\beta_2 x_8$$

$$\dot{x}_5 = \frac{1}{C_{\mathrm{s}1}} x_4 - \frac{1}{C_{\mathrm{s}1}} x_6$$

$$\dot{x}_6 = \frac{1}{L_1} x_5 - \frac{R_1}{L_1} x_6 - \frac{1}{L_1} x_{10}$$

$$\dot{x}_7 = \gamma\beta_2 x_2 - \gamma\beta_2 R_{\mathrm{P}} x_3 - \sigma_2\beta_1 R_{\mathrm{s}1} x_4 - \sigma_2\beta_1 x_5 - \alpha_2 x_7 - \eta_2 x_8$$

$$\dot{x}_8 = \frac{1}{C_{\mathrm{s}2}} x_7 - \frac{1}{C_{\mathrm{s}2}} x_9$$

$$\dot{x}_9 = \frac{1}{L_2} x_8 - \frac{R_2}{L_2} x_9 - \frac{1}{L_2} x_{10}$$

$$\dot{x}_{10} = \frac{1}{C} x_6 - \frac{1}{C} x_9 - \frac{1}{CR} x_{10}$$

Where

$$\beta_{\mathrm{j}} = \frac{M_{\mathrm{j}}}{L_{\mathrm{P}} L_{\mathrm{sj}}}, \gamma = \frac{1}{1 - \sum_{\mathrm{j}=1}^{2} M_{\mathrm{j}}\beta_{\mathrm{j}}}, \eta_{\mathrm{j}} = \frac{1 + \gamma\beta_{\mathrm{j}} M_{\mathrm{j}}}{L_{\mathrm{sj}}}$$

$$\alpha_{\mathrm{j}} = \frac{R_{\mathrm{sj}}(1 + \gamma\beta_{\mathrm{j}} M_{\mathrm{j}})}{L_{\mathrm{sj}}}, \sigma_{\mathrm{j}} = \frac{\gamma M_{\mathrm{j}}}{L_{\mathrm{sj}}}, \mathrm{j} = 1, 2$$

It can be expressed in the form of a state-space equation.

$$\dot{x} = Ax + Bu \tag{2.9}$$

The coefficient matrix A is given at the end of the paper. The input matrix B is given by:

$$B = \begin{bmatrix} \frac{1}{L} & 0 & 0 & 0 & 0 & 0 & 0 & 0 & 0 & 0 \end{bmatrix}^{\mathrm{T}}$$

Select the voltage across the load $u_c = x_{10}$ as the output, and the output equation can be written as:

$$y = Cx \tag{2.10}$$

The coefficient matrix C is given by:

$$C = \begin{bmatrix} 0 & 0 & 0 & 0 & 0 & 0 & 0 & 0 & 0 & 1 \end{bmatrix}$$

D. The Uncertainly System Model

There is an error between the dynamic model and the actual system, which is referred to as system uncertainties. The uncertainties can be divided into two categories: parameter uncertainties and unstructured uncertainties. In the ICPT system, the actual electrical parameters and theoretical parameters are inconsistent due to inaccuracy in the measuring device and manufacturing process. In order to approach the actual ICPT system, it is necessary to establish its uncertain mathematical model. Suppose the uncertainties of the ICPI system are

$$L_{\mathrm{p}} = L_{\mathrm{p}0} + \Delta L_{\mathrm{P}}, L_{\mathrm{s}1} = L_{\mathrm{s}10} + \Delta L_{\mathrm{s}1}, L_{\mathrm{s}2} = L_{\mathrm{s}20} + \Delta L_{\mathrm{s}2}$$

Where: L_{p0}、L_{S10} and L_{S20} are the nominal values of L_P、L_{S1} and L_{S2}, respectively, ΔL_P、ΔL_{S1} and ΔL_{S2} are the uncertainties of L_P、L_{S1} and L_{S2}, respectively.

By substituting the uncertain factors into (2.9) and (2.10), the mathematical model of the parameter uncertainties of the ICPT system can be expressed as follow:

$$\begin{cases} \dot{x} = A'x + B'u \\ y = C'x \end{cases} \tag{2.11}$$

Where: A′ is given at the end of the paper, $B'=B$, $C'=C$, ξ_1、ξ_2、ξ_3、ξ_4、ξ_5、ξ_6、ξ_7 are uncertainty parameters caused by uncertainty factors ΔL_P、ΔL_{S1} and ΔL_{S2}.

Let the uncertainty parameters satisfy the following conditions.

$$|\xi_1| \le 0.01, |\xi_2| \le 0.1, |\xi_3| \le 0.1, |\xi_4| \le 0.00015, |\xi_5| \le 0.5, |\xi_6| \le 0.5, |\xi_7| \le 0.00015$$

According to the uncertain mathematical model of the ICPT system, when the uncertainty factors change, the same type of uncertainty mathematical model of ICPT system can be obtained by changing the parameters representing the uncertainty factors.

III. The Design of Guaranteed Performance Controller

The dual-pickup ICPT system with D-LCL compensation has high-order resonance characteristics and is highly sensitive to parameter changes. To overcome the influence of parameter uncertainty factors on the system, some scholars have proposed robust H_∞ control, but its control requirements for uncertainties are limited to robust stability. The guaranteed performance controller based on linear matrix inequality (LMI) method can obtain robust performance while achieving robust stability.

A. Guaranteed Performance Control of Uncertainty System

Consider a class of linear uncertainty system described by the following state equation.

$$\dot{x}(t) = (A + \Delta A)x(t) + (B + \Delta B), x(0) = x_0 \quad (3.1)$$

Where $x(t) \in \mathrm{R}^n$ represents the state vector of the system. $u(t) \in \mathrm{R}^m$ is the control input. A and B are foregone and constant matrices with appropriate dimensions. ΔA and ΔB are uncertainty matrix functions with appropriate dimensions, and they represent the parameter uncertainties of the system. Assume that the parameter uncertainties considered are norm bounded and have the following form:

$$\begin{bmatrix} \Delta A & \Delta B \end{bmatrix} = DF(t)\begin{bmatrix} E_1 & E_2 \end{bmatrix} \quad (3.2)$$

Where D、E_1 and E_2 are known constant matrices with appropriate dimensions, which reflect the structural information of the uncertainties, $F \in \mathrm{R}^{i \times j}$ is an unknown matrix, which can be time-varying and satisfies (3.3).

$$F^{\mathrm{T}}(t)F(t) \le I \quad (3.3)$$

Define quadratic performance index as

$$J = \int_0^\infty \left[x^{\mathrm{T}}(t)Qx(t) + u^{\mathrm{T}}(t)Ru(t) \right] \mathrm{d}t \quad (3.4)$$

Where: Q and R are the given symmetric positive definite weighting matrices.

Theorem 3.1.(see[24]) *For the system (3.1) and the performance index (3.4), if the control law u*(t) and a positive number J* exist, the closed-loop system is asymptotically stable for the allowed uncertainty, and the performance index satisfies J≤J*. J* is called performance upper bound of the uncertain system (3.1), and u*(t) is called its guaranteed performance control law.*

Choose an appropriate guaranteed performance control law to minimize the system performance upper bound. The guaranteed performance control law with the minimum performance upper bound is called the optimal guaranteed performance control law.

B. The Design of Output Feedback Guaranteed Performance Controller of The Dual-pickup ICPT System with D-LCL Compensation

The equation for the uncertain system (2.11) can be transformed into

$$\begin{aligned} \dot{x}(t) &= (A + \Delta A)x(t) + (B + \Delta B)u(t), x(0) = x_0 \\ y(t) &= Cx(t) \end{aligned} \quad (3.5)$$

Where: ΔA is given at the end of the paper, ΔB=0.

Describe ΔA and ΔB, according to (3.2).

$$D = \Delta A, F(t) = I_{10}, E_1 = I_{10}, E_2 = 0$$

Design a dynamic output feedback controller with the following state-space implementation for the system (3.5), and it is shown as $u=Ky$.

$$\begin{aligned} \dot{x}_k(t) &= A_k x_k(t) + B_k y(t) \\ u(t) &= C_k x_k(t) \end{aligned} \quad (3.6)$$

Where: $x_k(t) \in \mathrm{R}^{nk}$ is the state of the controller to be designed, A_k, B_k and C_k are the controller parameter matrices to be determined.

The closed-loop system obtained by combining the controller (3.6) with the system (3.5) is as follow:

$$\begin{aligned} \dot{\bar{x}}(t) &= (\bar{A} + \bar{D}F(t)\bar{E})\bar{x}(t), \bar{x}(0) = \bar{x}_0 \\ \bar{y}(t) &= \bar{C}\bar{X} \end{aligned} \quad (3.7)$$

Where:

$$\bar{x}(t) = \begin{bmatrix} x(t) \\ x_k(t) \end{bmatrix}, \bar{A} = \begin{bmatrix} A & BC_k \\ B_k C & A_k \end{bmatrix}, \bar{D} = \begin{bmatrix} D \\ 0 \end{bmatrix}, \bar{E} = \begin{bmatrix} E_1 & 0 \end{bmatrix}, \bar{C} = \begin{bmatrix} C & 0 \end{bmatrix}$$

The performance function of the closed-loop system (3.7) is

$$J = \int_0^\infty \bar{x}^{\mathrm{T}}(t)\bar{Q}\bar{x}(t)\mathrm{d}t \quad (3.8)$$

Where: the performance weighting matrix is given by:

$$\bar{Q} = \mathrm{diag}\left\{ Q, C_k^{\mathrm{T}} R C_k \right\}$$

Theorem 3.2.(see [25]) *For the system (3.7) and the performance indicator (3.8), if there is a positive definite matrix P>0, then*

$$(\bar{A} + \bar{D}F\bar{E})^{\mathrm{T}} P + P(\bar{A} + \bar{D}F\bar{E}) + \bar{Q} < 0 \quad (3.9)$$

applies to all allowed uncertainties F(t), the positive definite matrix P is called the quadratic cost matrix.

Lemma 3.1.(see [25]) *Given system (3.7) and performance indicator (3.8), if there is a quadratic cost matrix P>0, then the uncertain system is quadratic stable, and the cost function is bounded and satisfies*

$$J < \bar{x}_0^{\mathrm{T}} P \bar{x}_0 .$$

Lemma 3.2.(see [25]) *The symmetric matrixes*

$$G, \bar{D}, F, \bar{E}$$

of the given appropriate dimensions are defined by (3.7). The necessary and sufficient condition for

$$G + \bar{D} F \bar{E} + \bar{E}^{\mathrm{T}} F^{\mathrm{T}} \bar{D}^{\mathrm{T}} < 0$$

to be established is that there is a scalar ε>0 so that

$$G + \begin{bmatrix} \varepsilon \bar{E}^{\mathrm{T}} & \varepsilon^{-1} \bar{D} \end{bmatrix} \begin{bmatrix} I & 0 \\ 0 & I \end{bmatrix}^{-1} \begin{bmatrix} \varepsilon \bar{E} \\ \varepsilon^{-1} \bar{D}^{\mathrm{T}} \end{bmatrix} < 0$$

Theorem 3.3. *For the system (3.7) and performance index (3.8), the necessary and sufficient condition for the existence of the quadratic cost matrix is that there is a scalar ε>0 and a positive definite matrix V>0 so that*

$$\begin{bmatrix} V\bar{A}^{\mathrm{T}} + \bar{A}V & V\bar{E}^{\mathrm{T}} & \bar{D} & V\bar{Q}^{1/2} \\ \bar{E}V & -I & 0 & 0 \\ \bar{D}^{\mathrm{T}} & 0 & -I & 0 \\ \bar{Q}^{1/2}V & 0 & 0 & -\varepsilon I \end{bmatrix} < 0 \tag{3.10}$$

Proof. According to Theorem 3.2, for all allowed uncertainties $F(t)$, the quadratic cost matrix P satisfies (3.9). It can be seen from Lemma 3.2 that the necessary and sufficient condition for (3.9) to be established is that there is a scalar $\varepsilon_1>0$ so that

$$\bar{A}^{\mathrm{T}} P + P\bar{A} + \bar{Q} + \begin{bmatrix} \varepsilon_1 \bar{E}^{\mathrm{T}} & \varepsilon_1^{-1} \bar{D} \end{bmatrix} \begin{bmatrix} I & 0 \\ 0 & I \end{bmatrix}^{-1} \begin{bmatrix} \varepsilon_1 \bar{E} \\ \varepsilon_1^{-1} \bar{D}^{\mathrm{T}} \end{bmatrix} < 0$$

Use Schur complement lemma to get

$$\begin{bmatrix} \bar{A}^{\mathrm{T}} P + P\bar{A} + \bar{Q} & \varepsilon_1 \bar{E}^{\mathrm{T}} & \varepsilon_1^{-1} P \bar{D} \\ \varepsilon_1 \bar{E} & -I & 0 \\ \varepsilon_1^{-1} \bar{D}^{\mathrm{T}} P & 0 & -I \end{bmatrix} < 0 \cdot$$

Multiply diag$\{\varepsilon_1 P^{-1}, I, I\}$ to the left and right sides of the above formula, and let $\varepsilon=\varepsilon_1^2$, $V=\varepsilon P^{-1}$, the following expression can be obtained:

$$\begin{bmatrix} V\bar{A}^{\mathrm{T}} + \bar{A}V + \varepsilon^{-1} V\bar{Q}V & V\bar{E}^{\mathrm{T}} & \bar{D} \\ \bar{E}V & -I & 0 \\ \bar{D}^{\mathrm{T}} & 0 & -I \end{bmatrix} < 0$$

Use Schur supplement lemma again to get

$$\begin{bmatrix} V\bar{A}^{\mathrm{T}} + \bar{A}V & V\bar{E}^{\mathrm{T}} & \bar{D} & V\bar{Q}^{1/2} \\ \bar{E}V & -I & 0 & 0 \\ \bar{D}^{T} & 0 & -I & 0 \\ \bar{Q}^{1/2}V & 0 & 0 & -\varepsilon I \end{bmatrix} < 0$$

Where:

$$\bar{Q}^{1/2} = \mathrm{diag}\{Q^{1/2}, C_k{}^{\mathrm{T}} R^{1/2}\} .$$

If V and ε exist, the upper bound of the corresponding performance indicator is

$$J < \varepsilon \bar{x}_0^{\mathrm{T}} V^{-1} \bar{x}_0 .$$

Theorem 3.4. *For the given system (3.5) and performance function (3.8), the necessary and sufficient condition for the existence of output feedback guaranteed performance controller (3.6) is that the following (3.11) and (3.12) are achievable.*

$$\begin{bmatrix} \Phi_1 & A' + A^{\mathrm{T}} & E_1{}^{\mathrm{T}} & XD & Q^{1/2} & 0 \\ A + A'^{\mathrm{T}} & \Phi_2 & YE_1 & D & YQ^{1/2} & C'^{\mathrm{T}} R^{1/2} \\ E_1 & E_1{}^{\mathrm{T}} Y & -I & 0 & 0 & 0 \\ D^{\mathrm{T}} X & D^{\mathrm{T}} & 0 & -I & 0 & 0 \\ Q^{1/2} & Q^{1/2} Y & 0 & 0 & -\varepsilon I & 0 \\ 0 & R^{1/2} C' & 0 & 0 & 0 & -\varepsilon I \end{bmatrix} < 0 \tag{3.11}$$

$$\begin{bmatrix} X & I \\ I & Y \end{bmatrix} > 0 \tag{3.12}$$

Where

$$\Phi_1 = A^{\mathrm{T}} X + XA + B'C + C^{\mathrm{T}} B'^{\mathrm{T}}, \Phi_2 = AY + YA^{\mathrm{T}} + BC' + C'^{\mathrm{T}} B^{\mathrm{T}} .$$

Proof. The variable substitution method proposed in [20] is used for (3.10) to block the matrices V and V^{-1}, we get

$$V = \begin{bmatrix} Y & N \\ N^{\mathrm{T}} & Y_1 \end{bmatrix}, V^{-1} = \begin{bmatrix} X & M \\ M^{\mathrm{T}} & X_1 \end{bmatrix}$$

Where: X and Y are both $n \times n$ dimensional real symmetric matrices, $MN^{\mathrm{T}}=I-XY$ can be obtained from the equation $VV^{-1}=I$.

Define

$$F_1 = \begin{bmatrix} X & I \\ M^{\mathrm{T}} & 0 \end{bmatrix}, F_2 = \begin{bmatrix} I & Y \\ 0 & N^{\mathrm{T}} \end{bmatrix},$$

then

$$VF_1 = F_2, V^{\mathrm{T}} F_1 V = F_2^{\mathrm{T}} F_1 = \begin{bmatrix} X & I \\ I & Y \end{bmatrix}.$$

Define the following new variables.

$$\begin{aligned} A^{'} &= XAY + B^{'}CY + XBC^{'} + MA_k N^{\mathrm{T}} \\ B^{'} &= MB_k \\ C^{'} &= C_k N^{\mathrm{T}} \end{aligned} \tag{3.13}$$

From the definition of V, F_1 and F_2 and (3.13), we can get

$$\begin{aligned} F_1^{\mathrm{T}} V \bar{A}^{\mathrm{T}} F_1 &= \begin{bmatrix} A^{\mathrm{T}} X + C^{\mathrm{T}} B^{\mathrm{T}} & A^{\mathrm{T}} \\ A^{\mathrm{T}} & YA^{\mathrm{T}} + C^{'\mathrm{T}} B^{\mathrm{T}} \end{bmatrix}, \\ F_1^{\mathrm{T}} \bar{A} V F &= \begin{bmatrix} XA + B^{'}C & A^{'} \\ A & AY + BC^{'} \end{bmatrix}, \\ \bar{E} V F_1 &= \begin{bmatrix} E_1 & E_1 Y \end{bmatrix}, \bar{D}^{\mathrm{T}} F = \begin{bmatrix} D^{\mathrm{T}} X & D^{\mathrm{T}} \end{bmatrix}, \\ \bar{Q}^{1/2} V F_1 &= \begin{bmatrix} Q^{1/2} & Q^{1/2} Y \\ 0 & R^{1/2} C^{'} \end{bmatrix} \end{aligned} \tag{3.14}$$

Multiply the left and right sides of (3.10) by diag$\{F_1^{\mathrm{T}}, I, I, I\}$ and diag$\{F_1, I, I, I\}$, respectively.

$$\begin{bmatrix} F_1^{\mathrm{T}} V \bar{A}^{\mathrm{T}} F_1 + F_1^{\mathrm{T}} \bar{A} V F_1 & F_1^{\mathrm{T}} V \bar{E}^{\mathrm{T}} & F_1^{\mathrm{T}} \bar{D} & F_1^{\mathrm{T}} V \bar{Q}^{1/2} \\ \bar{E} V F_1 & -I & 0 & 0 \\ \bar{D}^{\mathrm{T}} F_1 & 0 & -I & 0 \\ \bar{Q}^{1/2} V F_1 & 0 & 0 & -\varepsilon I \end{bmatrix} < 0 \tag{3.15}$$

Based on (3.14), the formula (3.15) can be transformed into (3.11). The implementation of

$$\begin{bmatrix} X & I \\ I & Y \end{bmatrix} > 0$$

is to ensure that $V>0$.

After using the LMI Control Toolbox in the MATLAB to find the feasible solutions of the linear matrix inequalities (3.11) and (3.12), we need to design the controller parameters.

(1) $MN^{\mathrm{T}}=I-XY$ is known, singular value decomposition is performed on $I-XY$, and the matrices M and N are calculated.

(2) The coefficient matrices of the controller can be obtained by (3.13).

$$\begin{aligned} A_k &= M^{-1}(A^{'} - XAY - B^{'}CY - XBC^{'})(N^{\mathrm{T}})^{-1} \\ B_k &= M^{-1} B^{'} \\ C_k &= C^{'}(N^{\mathrm{T}})^{-1} \end{aligned}$$

IV. Simulink

When setting parameters for the dual-pickup ICPT system based on D-LCL compensation, it is ensured that the entire resonant network is fully operated at the natural resonant frequency. Based on this principle, the system parameters are set, as shown in Table II.

TABLE II
PARAMETER SETTING OF DUAL-PICKUP ICPT SYSTEM BASED ON D-LCL COMPENSATION

Parameter	Value	Parameter	Value
f/kHz	20	C_{S1}/uF	0.916
L/uH	0.56	L_1/ uH	0.968
R_L/Ω	0.55	R_1/Ω	0.18
C_P/uF	1.23	L_{S2}/ uH	0.128
L_P/ uH	0.56	R_{S2}/Ω	0.18
R_P/Ω	0.55	C_{S2}/uF	0.916
M_1/uH	0.037	L_2/ uH	0.968
M_2/uH	0.037	R_2/Ω	0.18
L_{S1}/ uH	0.128	C/uF	1.017
R_{S1}/Ω	0.15	R/Ω	60

When the parameters shown in the above table are selected, the coefficient matrices of the system (3.5) are as follows: A, B and ΔA are given at the end of the paper.

Weighting matrices in performance index (3.5) are $Q=0.01I_{10}$ and $R=0.01$.

The linear matrix inequalities (3.11) and (3.12) are solved using the commands in the MATLAB LMI Control Toolbox to obtain the gain matrices of the output feedback controller. A_k, B_k and C_k are given at the end of the paper.

At this time, the upper limit of the system performance index: J≤0.503.

The same pulse input signal is provided to the closed-loop system with the nominal model which is composed of A and B and the uncertain model which is composed of A, ΔA, and B, we can get the impulse response curves of the system.

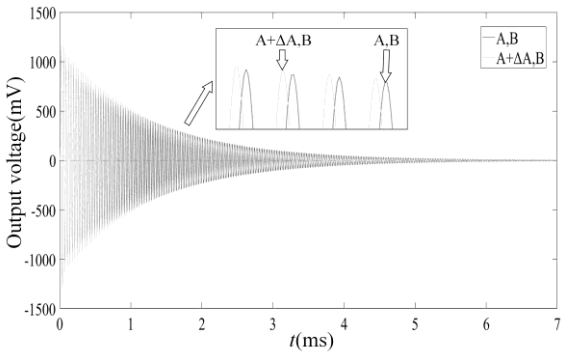

Fig. 10. Impulse response curve

Fig. 10 shows that the designed robust guaranteed performance controller ensures an excellent dynamic response of the output voltage across the load. The amplitude of the oscillation is large within 0.001s. There is about 0.004s to be spent for the load voltage to stabilize at 0V. Also, the parameter perturbations of the system model have little effect on the output response, and the control system has excellent robust stability.

V. Conclusion

In order to overcome the influence of parameters uncertainty on the dual-pickup ICPT system, this paper proposes an output feedback robust guaranteed performance controller. Firstly, for the dual-pickup ICPT system, the appropriate compensation topology: D-LCL is selected, and establishes the parameter uncertainty model. Then, the optimal output feedback guaranteed performance controller

for uncertainty system is designed by using the guaranteed performance control method, and the necessary and sufficient condition for the existence of the output feedback guaranteed performance controller is obtained. Finally, the LMI Toolbox in MATLAB is used to solve the gain matrices of the guaranteed performance controller and the upper bound of the system quadratic performance index, and the impulse response curves of the closed-loop system with the nominal and uncertain models are obtained. The simulation results show that the ICPT system controlled by this method has excellent robust stability and performance robustness, but it needs to be further studied in practical applications.

REFERENCES

[1] E. Abdelhamid, A. K. Abdelsalam, A. Massoud, and S. Ahmed, "An enhanced performance IPT based battery charger for electric vehicles application," in *2014 IEEE 23rd International Symposium on Industrial Electronics (ISIE)*, Turkey, 2014, pp.1610-1615.

[2] R. Mai, and S. Ma, "Research on Inductive Power Transfer Systems with Dual Pick-up Coils," *Proceedings of the CSEE*, vol. 49, no. 4, pp. 5192-5199, 2016.

[3] L. Ma, "Research on inductive power transfer technology based on multi-level and multi-receiver," Electrical Engineering, Southwest Jiaotong University, Sichuan, China, 2017.

[4] X. Dai, L. Li, X. Y. Yu, Y. L. Li, and Y. Sun, "A Novel Multi-Degree Freedom Power Pickup Mechanism for Inductively Coupled Power Transfer System," *IEEE Transactions on Magnetics*, vol. 53, no. 5, 2017.

[5] J. H. Kim, B. S. Lee, J. H. Lee, S. H. Lee, and C. B. Park, "Development of 1-MW Inductive Power Transfer System for a High-Speed Train," *IEEE Transactions on Industrial Electronics*, vol. 62, no. 10, pp. 6242-6250, 2015.

[6] A. Zaheer, D. Kacprzak, and G. A. Covic, "Bipolar Receiver Pad in a Lumped IPT System for Electric Vehicle Charging Applications," in *2012 IEEE Energy Conversion Congress and Exposition (ECCE)*, USA, 2012, pp.283-290.

[7] K. Song, C. B. Zhu, Y. Li, Y. Guo, J. H. Jiang, and J. T. Zhang, "Wireless Power Transfer Technology for Electric Vehicle Dynamic Charging Using Multi-parallel Primary Coils," *Proceeding of the CSEE*, vol. 35, no. 17, pp. 4445-4453, 2015.

[8] H. Wang, and X. Li, "Review and research progress of wireless power transfer for railway transportation," *IEEJ TRANSACTIONS ON ELECTRICAL AND ELECTRONIC ENGINEERING*, vol. 14, no. 3, pp. 475-484, 2019.

[9] S. Orike, and S. O. Alase, "Dynamic Wireless Power Transfer in Electric Vehicles using Magnetic Resonance: A Case of Developing Countries," in *Lecture Notes in Engineering and Computer Science: Proceedings of The World Congress on Engineering*, London, 2019, pp.198-202.

[10] M. Bertoluzzo, G. Buja, and H. K. Dashora, "Design of DWC System Track with Unequal DD Coil Set," *IEEE Transactions on Transportation Electrification*, vol. 3, no. 2, pp. 380-391, 2017.

[11] A. R. C. Cheah, K. H. Yeap, K. Hirasawa, K. C. Yeong, and H. Nisar, "Optimization of a Wireless Power Transmission System," in *Lecture Notes in Engineering and Computer Science: Proceedings of The International MultiConference of Engineers and Computer Scientists*, Hong Kong, 2016, pp.590-592.

[12] S. Y. Lin, and X. S. Huang, "Modelling and design of TS-S compensation networks for WPT system," *Journal of Fujian University of Technology*, vol. 14, no. 3, pp. 269-273, 2016.

[13] M. M. Zhao, Y. S. Li, J. R. Du, and J. Liu, "Hybrid compensation method and verification of ICPT system based on LCC topology," *Electrical Measurement & Instrumentation*, vol. 56, no.5, pp. 13-19, 2019.

[14] W. Dai, "Research on Low Voltage and High Power ICPT System Based on Double LCC Compensation," High voltage and insulation technology, Kunming University of Science and Technology, Kunming, China, 2018.

[15] Y. Li, L. Huang, Z. He, and Y. Liu, "Improved robust control for inductive power transfer system under parameters perturbations," *Electric Machines and Control*, vol. 20, no.7, pp. 40-48, 2016.

[16] Yan-Ling Li, Yue Sun, and Xin Dai, "Robust control for an uncertain LCL resonant ICPT system using LMI method," *Control Engineering Practice*, vol. 21, no.1, pp. 31-41, 2013.

[17] Lei Liu, Zejin Feng, Shaoying Lu, and Cunwu Han, "Optimal Guaranteed cost control for linear systems based on state feedback," in *29th Chinese Control and Decision Conference (CCDC)*, Chongqing, 2017, pp. 97-101.

[18] J. Y. Zhang, S. P. Ma, and Z. Kulan, "Guaranteed Cost Control of Uncertain Continuous-Time Singular Semi-markov Jump Systems with Indefinite Quadratic Cost via Static Output Feedback," in *37th Chinese Control Conference(CCC)*, Wuhan, 2018, pp.1469-1474.

[19] Y. X. Chen, and Y. C. Wang, "Study on Robust Guaranteed Cost Control for Linear Motor Servo System," *Proceedings of the CSEE*, vol. 26, no.24, pp. 174-179, 2006.

[20] G. M. Xu, and W. Q. Zhao, "Static output feedback guaranteed cost control for linear system," *Textile Dyeing and Finishing Journal*, vol. 38, no. 11, pp. 40-48, 2016.

[21] W. X. Liu, and W. Guo, "Design and Realization of H∞ Controllers Based on Riccati Equation and LMI Algorithm," *Computer Measurement & Control*, vol. 25, no. 2, pp. 74-76, 2017.

[22] Y. G. Wang. "Research on Control Algorithm Based on Inverted Pendulum System," Mechatronic Engineering, Xidian University, Xian, China, 2009.

[23] C. Y. Xia, X. Shao, Y. H. Li, K. Z. Lin, Z. P. Gu, and N. Lai, "Characteristic Research of ICPT System Based on Double LCL Structure for Achieving Constant Frequency, Constant Current and Stable Voltage Output," *Journal of Sichuan University (Engineering Science Edition)*, vol. 48, no. 3, pp. 156-163, 2016.

[24] Li. Yu, *Robust Control——Linear Matrix Inequality Processing*, Tsinghua University Press, Beijing, 2002, pp.41-60.

[25] D. W. Zhang, *Robust Analysis and Synthesis of Uncertain Systems——Matrix Inequality Method*, National Defense Industry Press, Beijing, 2014, pp.45-74.

$$A=\begin{bmatrix}
-\frac{R_L}{L} & -\frac{1}{L} & 0 & 0 & 0 & 0 & 0 & 0 & 0 & 0 \\
\frac{1}{C_P} & 0 & -\frac{1}{C_P} & 0 & 0 & 0 & 0 & 0 & 0 & 0 \\
0 & \frac{\gamma}{L_P} & -\frac{\gamma R_P}{L_P} & -\gamma\beta_1 R_{s1} & -\gamma\beta_1 & 0 & -\gamma\beta_2 R_{s2} & -\gamma\beta_2 & 0 & 0 \\
0 & \gamma\beta_1 & -\gamma\beta_1 R_P & -\alpha_1 & -\eta_1 & 0 & -\sigma_1\beta_2 R_{s2} & -\sigma_1\beta_2 & 0 & 0 \\
0 & 0 & 0 & \frac{1}{C_{s1}} & 0 & -\frac{1}{C_{s1}} & 0 & 0 & 0 & 0 \\
0 & 0 & 0 & 0 & \frac{1}{L_1} & -\frac{R_1}{L_1} & 0 & 0 & 0 & -\frac{1}{L_1} \\
0 & \gamma\beta_2 & -\gamma\beta_2 R_P & -\sigma_2\beta_1 R_{s1} & -\sigma_2\beta_1 & 0 & -\alpha_2 & -\eta_2 & 0 & 0 \\
0 & 0 & 0 & 0 & 0 & 0 & \frac{1}{C_{s2}} & 0 & -\frac{1}{C_{s2}} & 0 \\
0 & 0 & 0 & 0 & 0 & 0 & 0 & \frac{1}{L_2} & -\frac{R_2}{L_2} & -\frac{1}{L_2} \\
0 & 0 & 0 & 0 & 0 & \frac{1}{C} & 0 & 0 & \frac{1}{C} & -\frac{1}{CR}
\end{bmatrix}$$

$$A^{'}=\begin{bmatrix}
-\frac{R_{\mathrm{L}}}{L} & -\frac{1}{L} & 0 & 0 & 0 & 0 & 0 & 0 & 0 & 0\\
\frac{1}{C_{\mathrm{P}}} & 0 & -\frac{1}{C_{\mathrm{P}}} & 0 & 0 & 0 & 0 & 0 & 0 & 0\\
0 & \frac{\gamma}{L_{\mathrm{P}}}(1+\xi_1) & -\frac{\gamma R_{\mathrm{P}}}{L_{\mathrm{P}}}(1+\xi_1) & -\gamma\beta_1 R_{s1}(1+\xi_2) & -\gamma\beta_1(1+\xi_2) & 0 & -\gamma\beta_2 R_{s2}(1+\xi_3) & -\gamma\beta_2(1+\xi_3) & 0 & 0\\
0 & \gamma\beta_1(1+\xi_2) & -\gamma\beta_1 R_{\mathrm{P}}(1+\xi_2) & -\alpha_1(1+\xi_4) & -\eta_1(1+\xi_4) & 0 & -\sigma_1\beta_2 R_{s2}(1+\xi_5) & -\sigma_1\beta_2(1+\xi_5) & 0 & 0\\
0 & 0 & 0 & \frac{1}{C_{s1}} & 0 & -\frac{1}{C_{s1}} & 0 & 0 & 0 & 0\\
0 & 0 & 0 & 0 & \frac{1}{L_1} & -\frac{R_1}{L_1} & 0 & 0 & 0 & -\frac{1}{L_1}\\
0 & \gamma\beta_2(1+\xi_3) & -\gamma\beta_2 R_{\mathrm{P}}(1+\xi_3) & -\sigma_2\beta_1 R_{s1}(1+\xi_6) & -\sigma_2\beta_1(1+\xi_6) & 0 & -\alpha_2(1+\xi_7) & -\eta_2(1+\xi_7) & 0 & 0\\
0 & 0 & 0 & 0 & 0 & 0 & \frac{1}{C_{s2}} & 0 & -\frac{1}{C_{s2}} & 0\\
0 & 0 & 0 & 0 & 0 & 0 & 0 & \frac{1}{L_2} & -\frac{R_2}{L_2} & -\frac{1}{L_2}\\
0 & 0 & 0 & 0 & 0 & \frac{1}{C} & 0 & 0 & \frac{1}{C} & -\frac{1}{CR}
\end{bmatrix}$$

$$\Delta A=\begin{bmatrix}
0 & 0 & 0 & 0 & 0 & 0 & 0 & 0 & 0 & 0\\
0 & 0 & 0 & 0 & 0 & 0 & 0 & 0 & 0 & 0\\
0 & \frac{\gamma}{L_{\mathrm{P}}}\xi_1 & -\frac{\gamma R_{\mathrm{P}}}{L_{\mathrm{P}}}\xi_1 & -\gamma\beta_1 R_{s1}\xi_2 & -\gamma\beta_1\xi_2 & 0 & -\gamma\beta_2 R_{s2}\xi_3 & -\gamma\beta_2\xi_3 & 0 & 0\\
0 & \gamma\beta_1\xi_2 & -\gamma\beta_1 R_{\mathrm{P}}\xi_2 & -\alpha_1\xi_4 & -\eta_1\xi_4 & 0 & -\sigma_1\beta_2 R_{s2}\xi_5 & -\sigma_1\beta_2\xi_5 & 0 & 0\\
0 & 0 & 0 & 0 & 0 & 0 & 0 & 0 & 0 & 0\\
0 & 0 & 0 & 0 & 0 & 0 & 0 & 0 & 0 & 0\\
0 & \gamma\beta_2\xi_3 & -\gamma\beta_2 R_{\mathrm{P}}\xi_3 & -\sigma_2\beta_1 R_{s1}\xi_6 & -\sigma_2\beta_1\xi_6 & 0 & -\alpha_2\xi_7 & -\eta_2\xi_7 & 0 & 0\\
0 & 0 & 0 & 0 & 0 & 0 & 0 & 0 & 0 & 0\\
0 & 0 & 0 & 0 & 0 & 0 & 0 & 0 & 0 & 0\\
0 & 0 & 0 & 0 & 0 & 0 & 0 & 0 & 0 & 0
\end{bmatrix}$$

$$A=\begin{bmatrix}
-9.82e^5 & -1.79e^6 & 0 & 0 & 0 & 0 & 0 & 0 & 0 & 0\\
8.13e^5 & 0 & -8.13e^5 & 0 & 0 & 0 & 0 & 0 & 0 & 0\\
0 & 1.86e^6 & -1.02e^6 & -8.12e^4 & -5.42e^5 & 0 & -8.12e^4 & -5.42e^5 & 0 & 0\\
0 & 5.42e^5 & -2.98e^5 & -1.20e^6 & -7.97e^6 & 0 & -2.37e^4 & -1.58e^5 & 0 & 0\\
0 & 0 & 0 & 1.09e^6 & 0 & -1.09e^6 & 0 & 0 & 0 & 0\\
0 & 0 & 0 & 0 & 1.03e^6 & -1.86e^5 & 0 & 0 & 0 & 0\\
0 & 5.42e^5 & -2.98e^5 & -2.37e^4 & -1.58e^5 & 0 & -1.20e^5 & -7.97e^6 & 0 & 0\\
0 & 0 & 0 & 0 & 0 & 0 & 1.09e^6 & 0 & -1.09e^6 & 0\\
0 & 0 & 0 & 0 & 0 & 0 & 0 & 1.03e^6 & -1.86e^5 & -1.03e^6\\
0 & 0 & 0 & 0 & 0 & 9.83e^5 & 0 & 0 & 9.83e^5 & -1.64e^4
\end{bmatrix}$$

$$B=\begin{bmatrix}1.79e^6 & 0 & 0 & 0 & 0 & 0 & 0 & 0 & 0 & 0\end{bmatrix}^{\mathrm{T}}$$

$$\Delta A = \begin{bmatrix} 0 & 0 & 0 & 0 & 0 & 0 & 0 & 0 & 0 & 0 \\ 0 & 0 & 0 & 0 & 0 & 0 & 0 & 0 & 0 & 0 \\ 0 & 1.86e^{4} & -1.02e^{4} & -8.12e^{3} & -5.42e^{4} & 0 & -8.12e^{3} & -5.42e^{4} & 0 & 0 \\ 0 & 5.42e^{4} & -2.98e^{4} & -179.33 & -1.20e^{3} & 0 & -1.18e^{4} & -7.90e^{4} & 0 & 0 \\ 0 & 0 & 0 & 0 & 0 & 0 & 0 & 0 & 0 & 0 \\ 0 & 0 & 0 & 0 & 0 & 0 & 0 & 0 & 0 & 0 \\ 0 & 5.42e^{4} & -2.98e^{4} & -1.18e^{4} & -7.90e^{4} & 0 & -179.33 & -1.20e^{3} & 0 & 0 \\ 0 & 0 & 0 & 0 & 0 & 0 & 0 & 0 & 0 & 0 \\ 0 & 0 & 0 & 0 & 0 & 0 & 0 & 0 & 0 & 0 \\ 0 & 0 & 0 & 0 & 0 & 0 & 0 & 0 & 0 & 0 \end{bmatrix}$$

$$A_k = \begin{bmatrix} 9.42e^{4} & -1.90e^{4} & 17.45 & 33.12 & 2.22 & 0.13 & 6.26 & 0.47 & 0.04 & 8.22e^{-4} \\ 5.83e^{7} & -4.25e^{5} & -8.94e^{3} & 1.95e^{3} & 127.44 & 7.63 & 369.01 & 27.16 & 2.09 & 0.05 \\ -2.18e^{9} & 1.81e^{8} & -1.70e^{6} & 5.91e^{4} & 2.48e^{3} & 153.41 & 1.12e^{4} & 527.87 & 42.12 & 0.85 \\ 1.02e^{10} & 2.48e^{8} & -3.55e^{7} & -1.85e^{7} & -9.77e^{5} & -3.31e^{4} & -3.3e^{6} & -1.20e^{5} & -1.03e^{4} & -220.41 \\ -8.01e^{10} & 2.12e^{8} & 6.34e^{8} & 3.34e^{8} & 2.50e^{6} & -3.84e^{5} & 5.95e^{7} & 6.34e^{5} & 8.59e^{4} & 1.97e^{3} \\ 3.76e^{12} & 1.81e^{11} & -1.42e^{10} & -6.79e^{9} & -3.41e^{8} & -2.33e^{7} & -1.28e^{9} & -7.29e^{7} & -6.38e^{6} & -2.14e^{5} \\ 5.40e^{10} & 1.31e^{9} & -1.88e^{8} & -9.37e^{7} & -2.98e^{6} & -1.99e^{5} & -1.85e^{7} & 2.50e^{6} & -4.80e^{4} & -1.17e^{3} \\ -3.76e^{11} & 9.97e^{8} & 2.97e^{9} & 1.48e^{9} & 1.40e^{7} & 1.47e^{6} & 2.97e^{8} & -2.64e^{8} & -4.95e^{5} & 9.26e^{3} \\ 1.37e^{13} & 6.61e^{11} & -5.17e^{10} & -2.47e^{10} & -1.25e^{9} & -8.46e^{7} & -4.68e^{9} & 1.65e^{10} & -2.33e^{7} & -7.80e^{5} \\ -6.06e^{14} & -4.71e^{13} & 1.95e^{12} & 8.80e^{11} & -7.73e^{10} & 5.45e^{9} & 1.66e^{11} & -2.70e^{5} & 1.50e^{9} & 3.67e^{7} \end{bmatrix}$$

$$B_k = \begin{bmatrix} -5.26e^{-4} & -0.04 & -2.79 & -44.39 & 2.18e^{4} & -5.15e^{5} & -234.75 & 1.02e^{5} & -1.88e^{6} & -8.20e^{6} \end{bmatrix}^{\mathrm{T}}$$

$$C_k = \begin{bmatrix} 8.16e^{9} & 1.83e^{6} & -1.44e^{6} & -4.94e^{5} & -3.43e^{4} & -1.95e^{3} & -9.34e^{4} & -7.32e^{4} & -535.62 & -12.45 \end{bmatrix}$$